LES OF TURBULENT UNDER-EXPANDED HYDROGEN JET FLAMES

Gallen, L.[1], Livebardon, T.[2] and Sommerer, Y.[2]

[1] Airbus Protect SAS, 37 Avenue Escadrille Normandie Niemen, 31700 Blagnac, France
lucien.gallen@airbus.com
[2] Airbus Operations SAS, 316 Route de Bayonne, 31300 Toulouse, France

Abstract

In the frame of hydrogen-powered aircraft, Airbus wants to understand all the H2 physics and explore every scenario in order to develop and manufacture safe products operated in a safe environment. Within the framework of a Large Eddy Simulation (LES) methodology for modeling turbulence, a comparative numerical study of free under-expanded jet H2/AIR flame is conducted. The investigated geometry consists of straight nozzles with a millimetric diameter fed with pure H2 at upstream pressures ranging from 2 to 10 bar. Numerical results are compared with available experimental measurements such as; temperature signals using thermocouples. LES confirms its prediction capability in terms of shock jet structure and flame length. A particular attention is paid for capturing experimental unstable flame when upstream pressure decreases. Furthermore, flame stabilization and flame anchoring are analyzed. Mechanisms of flame stabilization are highlighted for case 1 and stabilization criteria are tested. Finally an ignition map to reach flame stabilization is proposed for each case regarding the literature.

Introduction

With the requirements of low-carbon transportation and green development, hydrogen has shown its potential to decarbonize parts of industry [1]. In this context, Airbus ambitions to develop the world's first hydrogen powered commercial aircraft by 2035. However, hydrogen has specific properties including low molar mass, lack of odor and color, and an extended flammability domain compared to kerosene [2,3]. Therefore specific safety analysis must be carried out. Because of its low density, hydrogen must be stored either in a gaseous state in vessels under high-pressure or in liquid state at a very low temperature in insulated tanks. Independently of storage, hydrogen must be distributed to the propulsion unit where it is used in gaseous form. Review of past hydrogen incidents [4] shows that one of the most common release scenarios involves leaks from these pressurized hydrogen-handling equipment. These leaks range from small-diameter, slow-release leaks originating from holes in piping or from accidental breaks in high-pressure tanks. The resulting hydrogen fuel jet must be characterized in order to understand hydrogen dispersion and evaluate the ignition risk. In case of ignition, the consequence of the hydrogen combustion must be evaluated as well in order to ensure the product safety. Significant scientific databases on hydrogen fuel jet related topics are available in the literature [5,6,7,8,9]. It enables the development of correlations and numerical methodologies required to predict hydrogen leaks at the design stage to build adequate safety responses.
The focus of this study is the high-pressure gaseous leak of hydrogen. A common scenario with high-pressure gaseous leak of hydrogen is the ignition at the source leading to a non-premixed turbulent jet flame with the structure of a highly under-expanded jet due to pressure ratio.
Experimental data to characterize hydrogen leaks have led to useful correlations [10,11]. They are based on several assumptions and have been validated extensively in hydrogen dispersion scenarios.

When dealing with combustion, first order approach can give estimation based on numerous correlations but fail to describe underlying physical phenomena behind these non-premixed turbulent jet flames. They also fail to address representative aircraft configuration where the combustion could occur in more or less confined areas with cross-flow ventilation or wind. Computational Fluid Dynamics (CFD) with Reynolds-averaged Navier-Stokes (RANS) is a recognized design tool to investigate both non-reactive [12] and reactive [13] under-expanded jet, or to investigate leak hole shape [14]. However, it is well known that standard combustion RANS models usually fail in predicting detailed flame structure as well as complex phenomena like flame ignition or blow-off, flame lift-off and flame-wall interaction. With the rise of computing resources, large Large Eddy Simulations (LES) have become extensively used for basic and applied research [12,15]. It differs from usual RANS simulations because it solves large eddies fluctuations and then captures unsteady effects. LES enables the analysis of complex physical phenomena involving turbulence, combustion, and shock physics [12] encountered in turbulent non-premixed under-expanded jet flames. These under-expanded jet flames are characterized by their leak orifice diameter, leak orifice shape, pressure ratio, and the downstream thermodynamics conditions. These parameters influence flame stabilization such as blow-off which can be observed varying only one of these parameters [16].
The purpose of the present paper is to demonstrate the capability of LES to capture under-expanded jet flame stabilization. An experimental configuration to provide temperature measurements along the jet flame with our targeted pressure is used as a benchmark for the present LES. For a given leak orifice diameter, 3 different pressure ratios are computed to highlight stabilization mechanisms compared to the literature.

Under-expanded jet

The upstream pressure ratio to the ambient pressure investigated in this study are categorized as under-expanded jets. Under-expanded jet differs from a subsonic jet when the pressure at the end of a nozzle or a hole is higher than the ambient pressure, the so-called jet pressure ratio (JPR) [17]. The under-expanded jet usually exhibits 3 zones:

1. the nearfield zone
2. the transition zone
3. the farfield zone

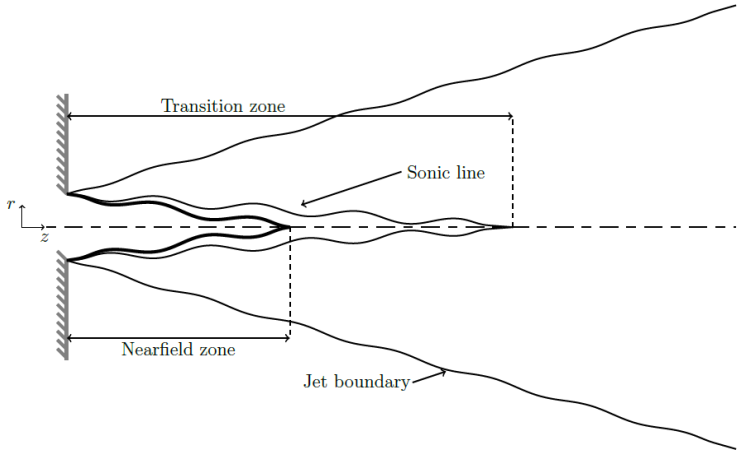

Figure 1: Schematic representation of under-expanded jet (extracted from [17])

Displayed in Fig. 1, the nearfield zone contains the supersonic core part and mixing layer. In the core part, the flow is isolated from the ambient fluid and its behavior is mainly dominated by compressible effects at high Mach number (>1). Compressible effects are characterized by successive isentropic expansion and compression of gas. A shearing zone between the sonic line and the jet boundary characterized by turbulent structures. Nearfield zone ends when the sonic line closes itself, it is the transition zone with small variations promoting mixing, pure H2 here and the ambient air through air entrainment in this zone. In the farfield zone, the jet is perfectly expanded (subsonic) and its characteristics are self-similar.

Experimental setup

In the Zero-E framework, Airbus led experimental campaigns in partnership with Ineris, the French national institute for Industrial Environment and risks, to gain knowledge in hydrogen torch fires from hydrogen leaks.
The experimental campaign consists of a moving high-pressure hydrogen pipe which delivers pure hydrogen in a non-confined environment at atmospheric conditions through a nozzle. Experimental measurements include a 3D flame temperature on a static grid with thermocouples (K type, 1mm diameter) and pressure measurements in the pipe upstream of the nozzle. The moving test bench and the fixed temperature measurement grid can be observed in Fig. 2.

Figure 2: Visualization of the test facility. Left: moving bench, right: nozzle and temperature measurement grid.

The rear view of the nozzle is shown in Fig. 3, the vertical instrument enables to evaluate the pressure in the nozzle upstream, ranging from 2 to 10 bar.

Figure 3: Nozzle rear view, pressure measurement instrumentation.

The high-pressure plug reference mimicking a hydrogen leak and its measurements are displayed in Fig. 4. It highlights the sudden restriction through the plug orifice.

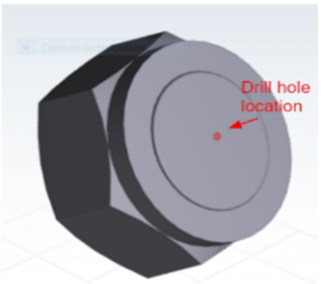

Figure 4: High Pressure plug reference.

Temperature measurements on the grid enable retrieval of the 2D experimental field of the free jet flame temperature. Two measurements are performed, 1) flame advances towards the grid, 2) flame moves back from the grid. It has been observed experimentally for the current facility that the H2 flame cannot stabilize for low pressure ratio ($1 < JPR < 2.1$) leading to flame extinction. This behavior, the influence of pressure on flame stabilization, will be investigated as well with numerical simulations.

Numerical setup

The CFD solver for the current study is AVBP developed by the CERFACS. AVBP is a suite of CFD tools to perform Direct Numerical Simulation (DNS) as well as LES of compressible, reacting, turbulent, multispecies flows (www.cerfacs.fr/avbp7x/). AVBP is perfectly set to handle flame stabilization with adequate models [18], for subsonic and supersonic flames [15,19]. AVBP is also used to compute deflagrations of H2-air mixture as well as H2 combustors [20,21,22]. LES set-up is similar to the one of Rochette et al. [18], except for chemistry modeling for which a semi-detailed SanDiego chemical mechanism is used [23] that comprises 9 transported species and 21 reactions. All computations are 3D and the spatial discretization is identical independently of the pressure ratio. Overall it counts 15M tetrahedral cells, with a minimum characteristic size of 50 µm inside the nozzle and near the H2-leak orifice ensuring axial velocity convergence along the axis. Then the spatial discretization is progressively decreased in the jet and set to 700µm in the jet flame. Each simulation case ran on 128 cores for 2 weeks.

In the near field zone, density gradients can be very stiff and lead to numerical acoustic oscillations. Localized Artificial Diffusivity (LAD), initially used for supercritical conditions [24], is chosen as a sensor based on the density gradients. It adds artificial viscosity in AVBP to damp oscillations in strong gradient regions in an appropriate manner.

Results and discussion

Three cases are investigated numerically varying the jet pressure ratio. The LES methodology is first validated for the first case with available temperature measurements. Then flame stabilization is investigated by the comparison of the three cases.

Case 1: Methodology validation

Figure 5 shows an instantaneous field of Mach number in non-reactive conditions. It corresponds to the near field supersonic zone which measures 35D, strong compression can be observed after the

Mach disk at 1D. The barrel shock in red indicates a highly under-expanded jet.

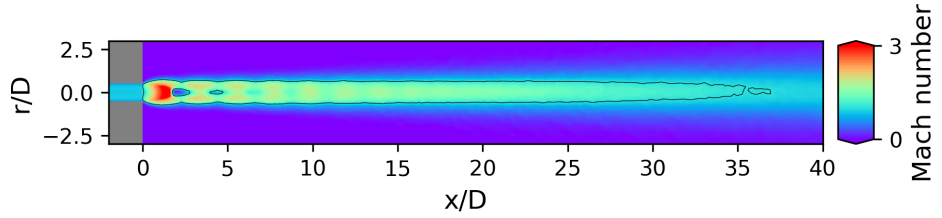

Figure 5: Instantaneous field of Mach number for the non-reactive case 1 simulation, with a black isoline Mach = 1.

An instantaneous field of H2 mass fraction is displayed in Fig. 6, a white isoline highlights the stoichiometric line while $X_{H2} = 11\%$ isoline is drawn in black revealing the lower ignition location [6]. Note that H2 field is limited to the flammable H2 region ($4\% < X_{H2} < 75\%$) to highlight jet dispersion. Mixing takes place around the supersonic zone in the shear layer with formation of vortices. Turbulence fluctuations begin around 75D inducing a strong and large mixing region. Then the mixing decreases with air entrainment.

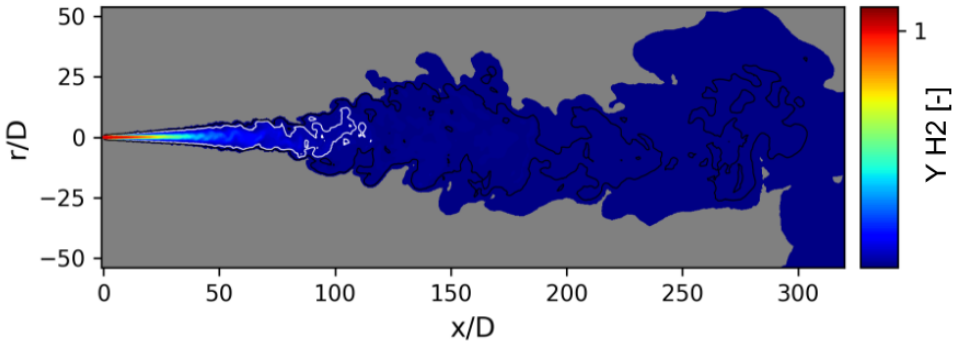

Figure 6: Instantaneous field of H2 mass fraction with stoichiometric line (white) and XH2 = 11% line (black) for case 1.

The mixture is ignited using a pocket of burnt gas along the stoichiometric line (in the mixture fraction-space). The flame is shown in Fig. 7 with an instantaneous field of temperature. The flame exhibits a thick stable flame along the supersonic zone, further downstream the flame front is thin at the end of the transition zone where turbulence begins. Then a strongly reactive turbulent flame takes place in the far field zone. The flame follows the stoichiometric line indicating mainly a diffusion combustion regime, assessed by the Takeno index [25] conditioned by heat release rate. Premixed combustion regime takes place at the end of the supersonic zone in the strong mixing region surrounded by a diffusion flame.

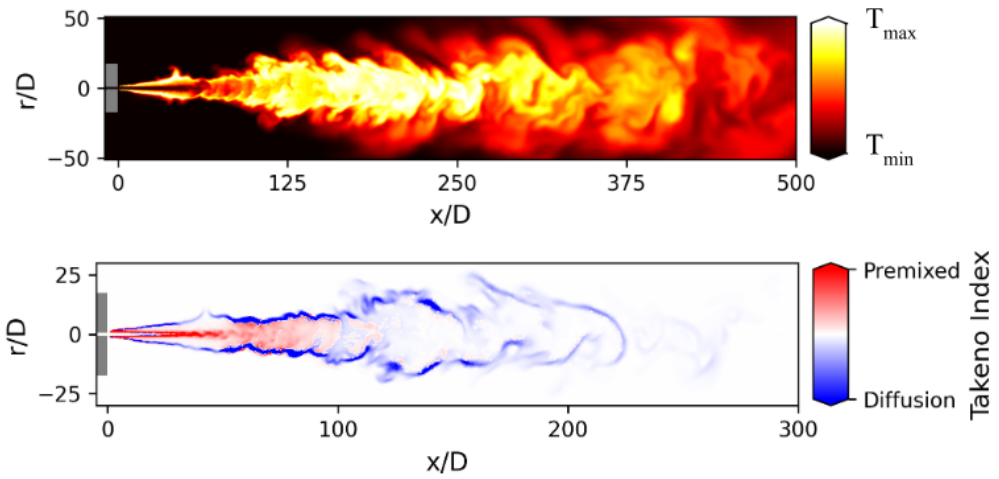

Figure 7: Instantaneous field of temperature (top) and Takeno index (bottom) for case 1.

Axial temperature at different locations are plotted in Fig. 8. The shift between the two experimental measurements (when the flame advances towards the grid and when the flame moves back from the grid) highlights the intrusive measurement technique. Although thermocouples are not recommended for turbulent flames, a good agreement along the axial axis x is observed with a good flame length, however a difference between thermocouples measurements and the numerical simulation is observed in the flame in the flame (x<400D). Temperature along axial direction at different radial locations (r = 0D, 50D and 100D) exhibits a good agreement. Experimental data suggests a larger flame opening, retrieved later at the end of the flame with LES. It can be explained by the apparition of turbulent vortices in the mixing layer which propagates downstream increasing jet opening. This turbulent activity is captured by the present LES, however the turbulent vortices are commonly computed in aeroacoustics [17]. In aeroacoustics, some guidelines have been proposed [26] for mesh refinement in larger nozzles but are not affordable in terms of computational cost for the current millimetric nozzle investigated .

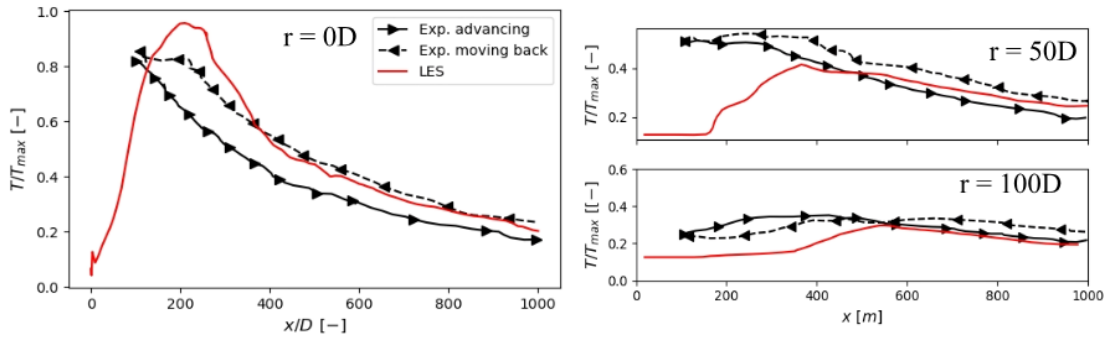

Figure 8: Comparison between numerical and measured temperature at origin r=0 (left) and r > 0 locations (right) in the axial direction.

Once the current methodology enables to retrieve flame length and flame temperature, LES can be analyzed to understand the underlying flame stabilization mechanisms. Mechanisms of flame stabilization in turbulent jet flames have been studied by Schefer and Goix [27], they generally rely on local ignition, flame propagation upstream, extinction and reignition phenomena. In their work, they evaluate the triple-flame concepts as a lifted-flame flame stabilization in turbulent reacting flows, as shown experimentally by Muniz and Mungal a year before [28]. Triple-flames occur when a flame propagates through a fuel concentration gradient, the fuel/air mixture varies from a lean mixture to a rich mixture through a stoichiometric mixture at the center. Velocity measurement by particle imagery

velocimetry (PIV) of triple flames indicate that the flow streamlines diverge upstream of the propagating flame as shown in the right part of Fig. 9. Schefer and Goix [27] explained that the divergence is due to acceleration of the velocity component normal to the premixed flames branches, then the upstream flow velocity decelerates due to divergence as the flame is approached and reaches a value close to the premixed laminar flame speed S_L, at the flame leading edge.

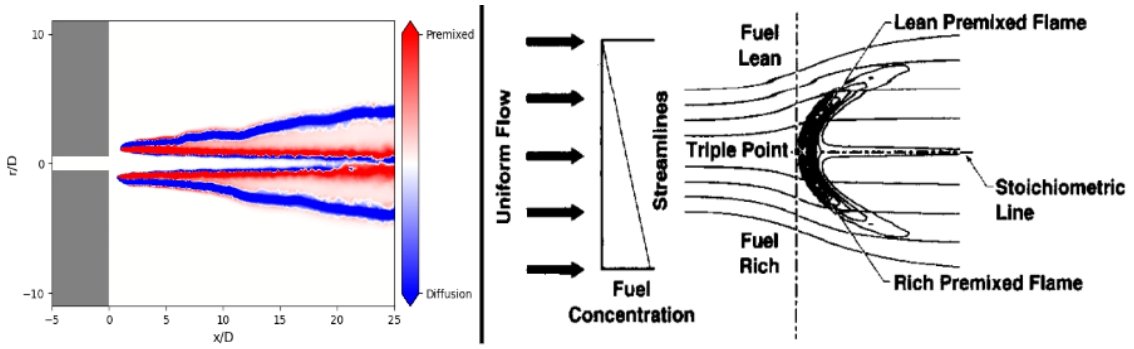

Figure 9: Instantaneous flame Takeno index conditioned by heat release close to the nozzle (left) and schematic triple-flame concept extracted from Schefer and Goix [26] (right).

Left part of Fig. 9 presents the Takeno index conditioned by heat release from Fig. 8 focusing on the near nozzle region. First of all, one can see that the flame is not anchored to the nozzle but slightly lifted about 1D, the size of the barrel shock.. At the flame root, a diffusion combustion front in blue is surrounded by two small premixed flames, a rich premixed flame on the supersonic jet side and a lean premixed flame on the other side. The current flame exhibits a triple-flame, and the triple-flame stability criteria stated by Muniz and Mungal can be applied. Based on the analysis of several flames burning different fuels, Muniz and Mungal proposed a criteria for flame stability: if upstream velocity (U) is lower than 3 laminar flame speed at stoichiometry (S_L) then the flame is able to propagate upstream and reach stability. This criteria is displayed with a black line indicating $3S_L$ value in Fig. 10, the field of temperature and the white stoichiometric line indicates the flame position. It shows that the flame position satisfies the present criteria in its stabilization region (< 50D), then the flame goes turbulent.

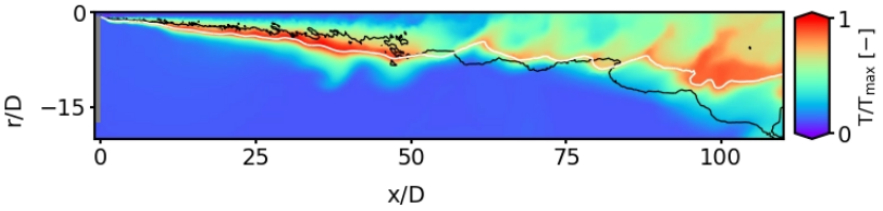

Figure 10: Half section of an instantaneous field of temperature with the stoichiometric line (white) and the triple-flame stability criteria 3 S_L line (black).

Flame stabilization

Two additional cases with lower pressure than the case 1 (P_1) are considered in this part: $P_1 > P_2 > P_3$. Experimental extinction has been observed for case 2 (P_2) after stopping the ignition source. Recently, Yamamoto et al [16] have measured blow-off of under-expanded jet flames for several jet pressure ratios and leak orifice diameter. They provide experimental results about under-expanded jet flame blow-off and concatenate a lot of experimental works found in the literature. This work leads to an useful diagram giving insights about flame blow-off depending on the reservoir pressure and nozzle diameter. It shows that varying one of the two parameters can lead to a flame blow-off. For small nozzle diameter, lower than 1 mm, blow-off limit is very close to the pressure of moderate/high

under-expanded jet flame studied in this work. A variation of pressure may be sufficient to reach blow-off conditions. An additional outcome of their work is a blow-off criteria based on the flame base position H_{fb} and the maximum waistline position H_{wl} of the stoichiometric contour where the radial direction is maximum. Yamamoto et al. [16] argue that if $H_{fb} < H_{wl}$ the flame is stable, unstable otherwise.

In this work, 3 S_L [28] and $H_{fb}<H_{wl}$ [16] are applied to the 3 cases. First of all, decreasing pressure leads to different under-expanded jets as observed for the non-reactive case in Fig. 11. Left part present a schlieren visualization in the near field region of the jet, one can see that we move from a well-described barrel shock (P_1) to a diamond shock structure (P_3) indicating the transition from a highly under-expanded jet to a moderate under-expanded jet. However, similar mixing in the shear layer region is observed for all cases. It is confirmed by the right part, showing the Mach number in the near field region, the strong disk Mach decreases with pressure until complete disappearance. It slightly affects the radial expansion of the first shock, but not the mixing process. The intensity of Mach number and the length of the supersonic zone decreases as well as the reservoir pressure decreases.

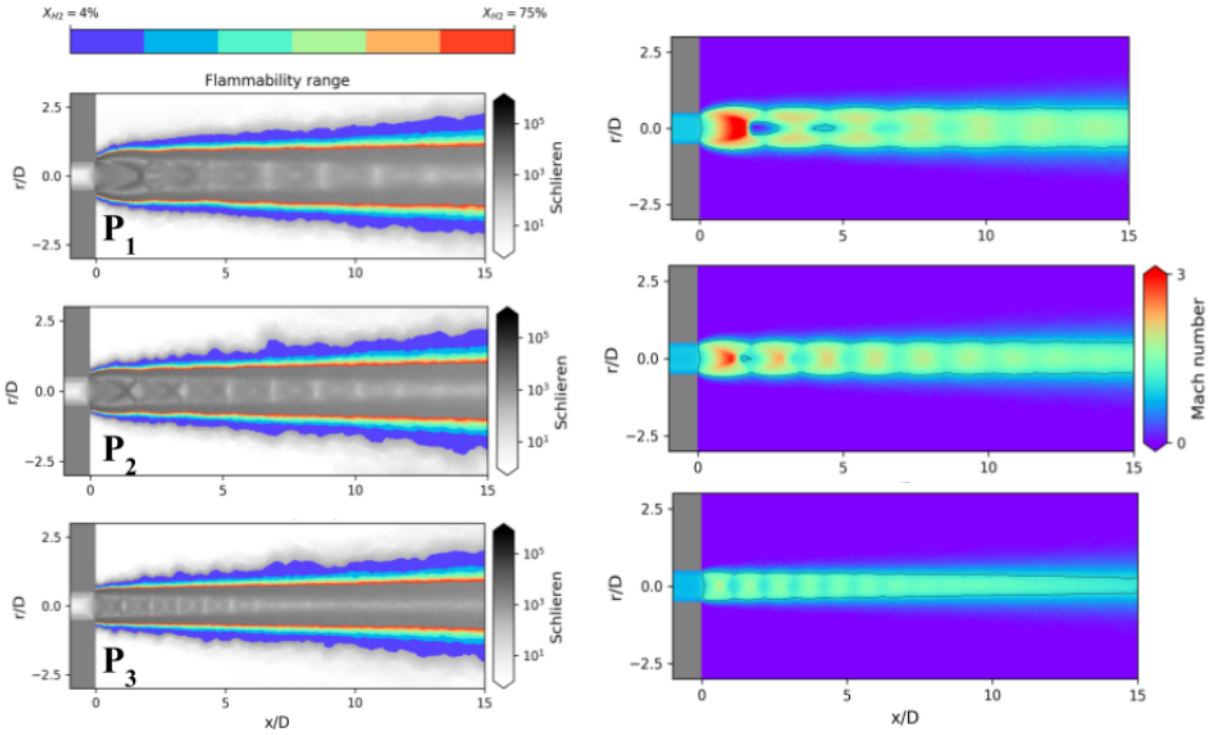

Figure 11: Instantaneous field of Schlieren and H2 molar fraction (left) and mach number (right) in the near field region.

The average fields of H_2 mass fraction are displayed in Fig.12 with the stoichiometric line, the maximum stoichiometric waistline H_{wl} is represented by a vertical white dotted line. The comparison of H_2 mass fraction highlights the differences between cases in terms of jet penetration in the quiescent medium. For case 1, H_{wl} is smaller than 100D without experimental measurements, the reference is then the LES simulation for this case where H_{fb} is lower, about 1D. So the Yamamoto et al. criteria ensures a stable flame for P_1.

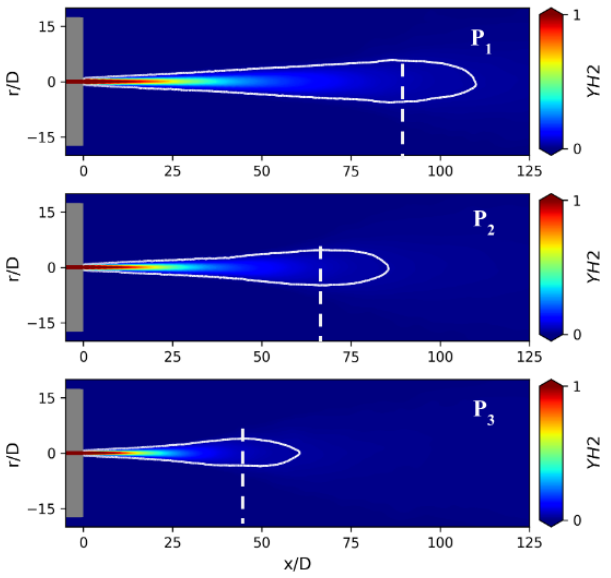

Figure 12: Mean field of H2 mass fraction with the white stoichiometric solid line for all cases. Stoichiometric waistline: vertical white dotted line.

When the flame is ignited in mixture fraction-space for the last two cases, similar flame position is observed in Fig. 13 where an instantaneous field of temperature is shown. First of all, the flame stabilizes successfully contrary to experimental observations for case P_2. Secondly, the flame reaches a similar H_{fb} than P_1 for both cases. Yamamoto et al. criteria predict stable behavior of the flame for all cases. Plotting $3S_L$ criteria shows that the flame reaches a stable region (<50D) similarly to the P_1 case where the flame stands on the correct side along the $3S_L$ line.

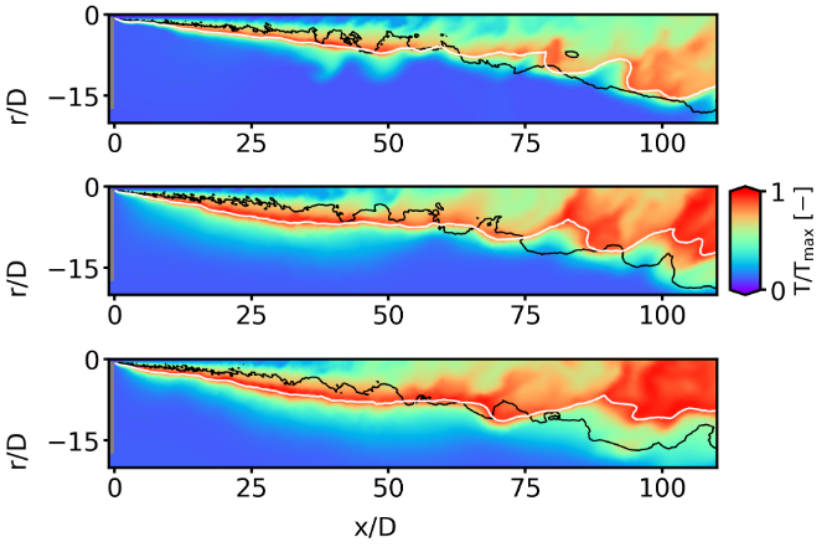

Figure 13: Mid section of instantaneous temperature field with stoichiometric line (white) and $3S_L$ stability criteria line (black).

The stability criteria investigated in this work are not able to understand the experimental flame behavior at P_2. The direct extinction after stopping ignition is similar to the so-called "Slow" region defined by Veser et al. [6] where the flame propagates only downstream the ignition source and quenches without ignition source. Veser et al. states that the flame propagates in both directions after ignition for X_{H2} > 11% and with local velocity lower than 60 m/s for hydrogen using a large

experimental database. The conclusions of Veser et al. allows us to map successful ignition from an non-reactive average solution as shown in Fig. 14. The green region without hatches (where velocity is too high) represents the ignition location for a successful flame propagation (upstream and downstream).

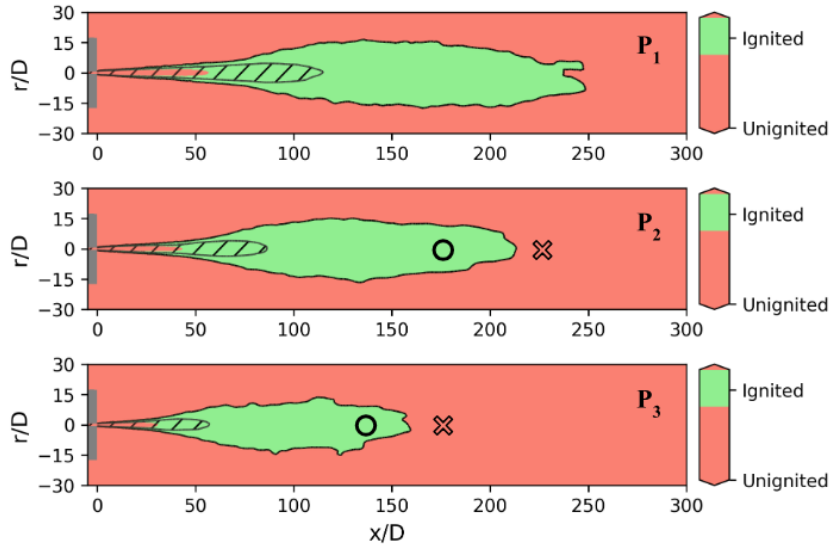

Figure 14: Mean map of successful ignition for all cases with Veser et al. criteria
Circles represent successful ignition location vs. direct extinction with an empty cross for P_2 and P_3.

The use of a more realistic ignition approach with a small spherical energy deposition for case P_2 and P_3 has been used. For each case, two ignition locations have been tested and reported in Fig. 14. One located in the green zone where upstream flame propagation is expected, the other is located at the boundary of this zone still in the hydrogen flammability range. Circles indicate that in LES flame successfully reaches the upstream region while cross indicates direction extinction after ignition source and then behaves similarly to the Veser et al. [6] observations.

Conclusions

High-fidelity numerical simulations of an experimentally characterized under-expanded hydrogen jet flame were conducted using an LES approach and a semi-detailed finite rate chemistry coupled with thickened flame model to take into account for flame-turbulence interactions. The approach leads to a reasonable agreement when comparing with available measurements such as temperature profiles along the axial direction. Once validated, a sensitivity analysis of the jet pressure ratio to the flame stabilization was conducted highlighting interesting behaviors already found in the literature. In particular, mechanisms driving flame stabilization as well as triple flame structure were then identified in the simulations. In the three investigated cases, similar mixing along the jet, favorable conditions for triple flame propagation and flame stabilization after ignition in the mixture-fraction space were observed suggesting stable conditions. The criteria proposed by Yamamoto et al. comparing flame lift-off and stoichiometric maximum waistline confirmed the flame stability predicted by LES. To go further with LES outputs, an ignition map was drawn with non-reactive simulations highlighting the ignition location where the flame can propagate both upstream and downstream. LES successfully captures the influence of the ignition location based on this map.
LES has shown its capability to predict under-expanded jet flames and to retrieve flame behavior observed in the literature considering flame ignition location. This LES-based methodology is promising to characterize such turbulent diffusion flame and its associated physics including flame lift-off, stabilization, shock-flame interactions, shocks induced turbulence. However, additional

numerical investigation with finer description of the jet supersonic coupled with well-characterized experimental study are still necessary.

Acknowledgements

The authors gratefully acknowledge CERFACS for their support to use the LES solver AVBP and their insights. The authors would also like to thank and acknowledge the contribution of Ineris for their valuable support for the experimental test campaign setup and realization. Funding from Airbus, DGAC and the European Union within the project NextGenerationEU is gratefully acknowledged.

References

[1] "The Future of Hydrogen – Analysis." *IEA*, 2019, https://www.iea.org/reports/the-future-of-hydrogen. Accessed 6 March 2023.
[2] Moradi, R. and Groth, K.M. "Hydrogen storage and delivery: Review of the state of the art technologies and risk and reliability analysis." *International Journal of Hydrogen Energy*, vol. 44, no. 23, 2019, pp. 12254-12269.
[3] Astbury, G. R. and Hawksworth, S. J.. "Spontaneous ignition of hydrogen leaks: A review of postulated mechanisms." *International Journal of Hydrogen Energy*, vol. 32, no. 13, 2007, pp. 2178-2185.
[4] Yang, F., Wang, T., Deng, X., Dang, J., Huang, Z., Hu, S., Li, Y. and Ouyang, M. "Review on hydrogen safety issues: Incident statistics, hydrogen diffusion, and detonation process." *International Journal of Hydrogen Energy*, vol. 46, no. 61, 2021, pp. 31467-31488.
[5] Schefer, R. W., Houf, W.G. and Williams, T.C. "Investigation of small-scale unintended releases of hydrogen: Buoyancy effects." *International Journal of Hydrogen Energy*, vol. 33, no. 17, 2008, pp. 4702-4712.
[6] Veser, A., Kuznetsov, M., Fast, G., Friedrich, A., Kotchourko, N. and Stern, G. "The structure and flame propagation regimes in turbulent hydrogen jets." *International Journal of Hydrogen Energy*, vol. 36, no. 3, 2011, pp. 2351-2359.
[7] Swain, M.R., Filoso, P.A. and Swain, M.N. "An experimental investigation into the ignition of leaking hydrogen." *International Journal of Hydrogen Energy*, vol. 32, no. 2, 2007, pp. 287-295.
[8] Schefer, R. W., Houf, W.G. and Williams, T.C. "Investigation of small-scale unintended releases of hydrogen: momentum-dominated regime." *International Journal of Hydrogen Energy*, vol. 33, no. 21, 2008, pp. 6373-6384.
[9] Han, S. H., Chang, D. and Kim, J.S. "Experimental investigation of highly pressurized hydrogen release through a small hole." *Experimental investigation of highly pressurized hydrogen release through a small hole*, vol. 39, no. 17, 2014, pp. 9552-9561.
[10] Houf, W. and Schefer, R. "Analytical and experimental investigation of small-scale unintended releases of hydrogen." *International Journal of Hydrogen Energy*, vol. 33, no. 4, 2008, pp. 1435-1444.
[11] Molkov, V.V. and Saffers, J.B. "Hydrogen jet flames." *International Journal of Hydrogen Energy,* vol. 38, no. 19, 2013, pp. 8141-8158.
[12] Hamzehloo, A. and Aleifiris, P. G. "LES and RANS modelling of under-expanded jets with application to gaseous fuel direct injection for advanced propulsion systems." *International Journal of Heat and Fluid Flow*, vol. 76, 2019, pp. 309-334.
[13] Benim, A. C. and Pfeiffelmann, B. "Comparison of Combustion Models for Lifted Hydrogen Flames within RANS Framework." *Energies*, vol. 13, no. 1, 2020.
[14] Stewart, J.R. "CFD modelling of underexpanded hydrogen jets exiting rectangular shaped openings." *Process Safety and Environmental Protection*, vol. 139, 2020, pp. 293-296.
[15] Boivin, P., Dauptain, A. and Cuenot, B. "Simulation of a supersonic hydrogen-air autoignition-stabilized flame using reduced chemistry." *Combustion and Flame*, vol. 159, no. 4, pp. 1779-1790.

[16] Yamamoto, S., Sakatsume, R. and Takeno, K. “Blow-off process of highly under-expanded hydrogen non-premixed jet flame.” *International Journal of Hydrogen Energy*, vol. 43, no. 10, 2018, pp. 5199-5205.
[17] Franquet, E., Perrier, V., Gibout, S. and Bruel, P. “Free underexpanded jets in a quiescent medium: A review.” *Progress in Aerospace Sciences*, vol. 77, 2015, pp. 25-53.
[18] Rochette, B., Collin-Bastiani, F., Gicquel, L., Vermorel, O., Veynante, D. and Poinsot, T. “Influence of chemical schemes, numerical method and dynamic turbulent combustion modeling on LES of premixed turbulent flames.” *Combustion and Flame*, vol. 191, 2018, pp. 417-430.
[19] Jaravel, T., Riber, E., Cuenot, B. and Pepiot, P. “Prediction of flame structure and pollutant formation of Sandia flame D using Large Eddy Simulation with direct integration of chemical kinetics.” *Combustion and Flame*, vol. 188, 2018, pp. 180-198.
[20] Dounia, O., Vermorel, O., Misdariis, A. and Poinsot, T. “Influence of kinetics on DDT simulations.” *Combustion and Flame*, vol. 200, 2019, pp. 1-14.
[21] Vermorel, O., Quillatre, P. and Poinsot, T. “LES of explosions in venting chamber: A test case for premixed turbulent combustion models.” *Combustion and Flame*, vol. 183, 2017, pp. 207-223.
[22] Aniello, A., Laera, D., Marragou, S., Magnes, H., Selle, L., Schuller, T. and Poinsot, T. “Experimental and numerical investigation of two flame stabilization regimes observed in a dual swirl H2 -air coaxial injector.” *Combustion and Flame*, vol. 249, 2023.
[23] Saxena, P. and Williams, F. “Testing a small detailed chemical-kinetic mechanism for the combustion of hydrogen and carbon monoxide.” *Combustion and Flame*, vol. 145, 2006, pp. 316-323.
[24] Schmitt, T. “Large-Eddy Simulations of the Mascotte test cases operating at supercritical pressure.” *Flow Turbulence and Combustion*, vol. 105, 2020, pp. 159-189.
[25] Yamashita, H., Shimada, M. and Takeno, T. “A numerical study on flame stability- at the transition point of jet diffusion flames.” *Proceedings of the Combustion Institute*, vol. 29, 1996, pp. 27-34.
[26] Liu, J., Kailasanath, K., Ramamurti, R., Munday, D., Gutmark, E. and Lohner, R. “Large-eddy simulations of a supersonic jet and its near-field acoustic properties.” *AIAA*, vol. 47, no. 8, 2009, pp. 1849-1865.
[27] Schefer, R. W. and P. J. Goix. “Mechanism of flame stabilization in turbulent lifted jet flames.” *Combustion and Flame*, vol. 112, 1998, pp. 559-574.
[28] Muniz, L. and Mungal, M. G. “Instantaneous flame-stabilization velocities in lifted-jet diffusion flames.” *Combustion and Flame*, vol. 111, 1997, pp. 16-30.